BRUKER

timsTOF Pro/fleX – Four reasons to switch to 4D-Proteomics™ on the timsTOF platform

If you are writing a grant and want some concise arguments for replacing older 3D mass spectrometers with the 4D capable on the timsTOF platform, download this brochure.

Click Here to Download the Brochure

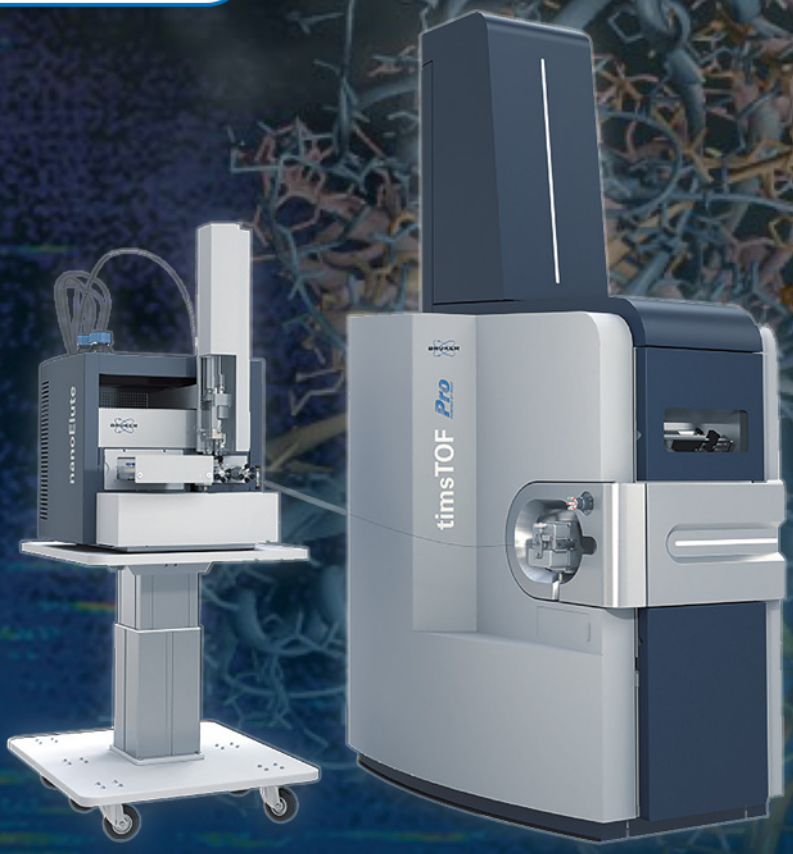

Proteomics
Proteomics and Systems Biology
www.proteomics-journal.com

DNA-Barcoded Fluorescence Microscopy for Spatial Omics

*Florian Schueder, Eduard M. Unterauer, Mahipal Ganji, and Ralf Jungmann**

Innovation in genomics, transcriptomics, and proteomics research has created a plethora of state-of-the-art techniques such as nucleic acid sequencing and mass-spectrometry-based proteomics with paramount impact in the life sciences. While current approaches yield quantitative abundance analysis of biomolecules on an almost routine basis, coupling this high content to spatial information in a single cell and tissue context is challenging. Here, current implementations of spatial omics are discussed and recent developments in the field of DNA-barcoded fluorescence microscopy are reviewed. Light is shed on the potential of DNA-based imaging techniques to provide a comprehensive toolbox for spatial genomics and transcriptomics and discuss current challenges, which need to be overcome on the way to spatial proteomics using high-resolution fluorescence microscopy.

1. Introduction

In order to understand the most fundamental principles of life, researchers have strived to develop novel techniques to detect, quantify, and spatially visualize interactions of proteins and nucleic acids on the level of single molecules in cells, tissues, and organisms using fluorescence microscopy. While current state-of-the-art single-molecule techniques offer unprecedented sensitivity to detect interactions of biomolecules,[1] they are usually limited to detect only a few molecular species at a time. Complexity of biological functions and processes inherently scales with the number of molecules involved, thus visualizing the interactions of just a handful of molecular species is insufficient to understand life's full complexity. In contrast, high content and quantitative abundance analysis of molecular species can be achieved using omics-type approaches such as genomics, transcriptomics, or proteomics. However, the spatial resolution of these techniques is rather limited.

Dr. F. Schueder, E. M. Unterauer, Dr. M. Ganji, Prof. R. Jungmann
Department of Physics and Center for Nanoscience
Ludwig Maximilian University
Geschwister-Scholl-Platz 1, Munich 80539, Germany
E-mail: jungmann@biochem.mpg.de
Dr. F. Schueder, E. M. Unterauer, Dr. M. Ganji, Prof. R. Jungmann
Max Planck Institute of Biochemistry
Am Klopferspitz 18, Martinsried 82152, Germany

The ORCID identification number(s) for the author(s) of this article can be found under https://doi.org/10.1002/pmic.201900368

DOI: 10.1002/pmic.201900368

Genomics and transcriptomics research techniques can be subdivided into de novo – for example, sequencing-based –readouts, providing relatively unbiased high-content information, or the analysis of known sequence motifs using nucleic acid probes developed to quantify the occurrence of these motifs in a relative or absolute fashion.[2,3] In proteomics research, a powerful quantification approach is mass spectrometry (MS), which allows to determine composition, stoichiometry, and topology of protein complexes.[4] These tools are well-suited for quantitative analysis. However, due to their workflow, which is traditionally based on the extraction of target molecules from cells or tissues, the spatial information provided by these assays is limited. To understand many cellular functions, spatial information is essential to put molecular abundance into the spatial context of a biological system in situ. With an ideal tool, it would be possible to detect all of these proximity interactions involved in cellular function with respect to their spatial location within a single cell and beyond.

In this review, we will focus on DNA-barcoded fluorescence microscopy for spatial omics. We discuss the potential of fluorescence microscopy as a future key player in spatial omics.

2. Current Approaches to Spatial Proteomics

While MS-based approaches are typically known for their capabilities in quantitative abundance analysis, they can also provide spatial information. One example of this regard is fractionated organelles post-lysis and protein–protein interaction network analysis.[5] Another exemplary approach uses antibodies for affinity purification of target proteins (called "baits") and their respective binding partners, followed by MS analysis.[5]

While these approaches provide a measure for spatial proximity, they are not capable of obtaining absolute spatial positions of proteins in single cells. In order to achieve this, cytometry-based imaging methods were developed (**Figure 1**a). Here, proteins of interest are stained with metal-labeled antibodies in tissue sections before they are subjected to either imaging mass cytometry (IMC)[6] or multiplexed ion beam imaging (MIBI)[7] for downstream analysis. In IMC, a high-resolution laser ablation system is used to transfer tissue material voxel-by-voxel into a cytometry by time-of-flight (CyTOF) mass cytometer to analyze the protein expression levels via metal isotope content (Figure 1b). In MIBI, an ion beam is used to scan over the tissue, generating secondary ions containing the metal isotopes bound to the antibodies. Using a sector mass spectrometer, the content of metal isotopes, and consequently protein expression levels are determined.

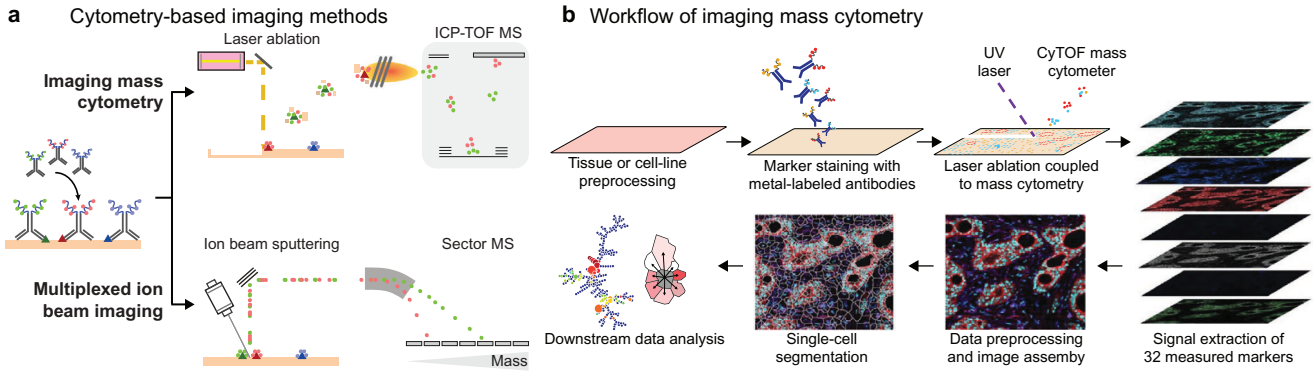

Figure 1. Cytometry-based imaging methods. a) Imaging mass cytometry. Tissue sections are stained by multiple, distinct metal-labeled antibodies. In cytometry by time-of-flight (CyTOF) imaging, laser ablation is used to obtain tissue sections, which are subsequently analyzed by CyTOF-MS to determine metal isotope content and thus epitope expression. In multiplexed ion beam imaging, a primary ion beam is used to raster over the tissue to generate secondary ions, among them the metal isotopes that were bound to the antibodies. A sector field mass spectrometer is then used to determine the metal isotope content and the associated epitope expression in each rastered area. Adapted with permission.[8] Copyright 2016, Elsevier. b) Workflow of imaging mass cytometry. After multiplexed metal-modified antibody labeling, the tissue is ablated in a voxel-style fashion and subsequently analyzed by a CyTOF mass cytometer. Combining the spatial information from the ablation process with the protein identity obtained from the CyTOF step, a spatially resolved, multiplexed "image" for up to 44 marker proteins is obtained, readying the data for downstream single-cell segmentation and analysis. Adapted with permission.[6] Copyright 2014, Springer Nature.

Although cytometry-based imaging methods can provide absolute spatial resolution and target multiplexing, they are currently limited by the precision of laser ablation and ion beam milling to about 200 nm spatial resolution.[8] Multiplexing in current implementations is limited due to the dependence on metal-modified antibodies to 44-plex.[8] Furthermore, the use of antibodies poses potential issues in terms of target labeling efficiency, specificity, and spatial accessibility, limiting quantitative analysis.

3. Fluorescence Microscopy as Potential Tool for Spatial Omics

While technical approaches described above provide exquisite high-content information, they struggle to obtain spatial information. To label and localize biomolecules in an absolute spatial context of complex cell and tissue environments, fluorescence tagging and imaging modalities such as fluorescence microscopy have been the major workhorses in life science research.[9,10] Its popularity is mainly based on three pillars: 1) relatively high spatial resolution, 2) multiplexed detection using spectrally distinct fluorophores, and 3) target specificity due to the ubiquitous availability of labeling reagents such as antibodies for proteins and DNA-based probes for nucleic acids, respectively.

However, if fluorescence microscopy ought to become a universally applicable spatial omics tool, these unique advantages are also its biggest achilles heel. First, the resolution of a conventional light microscope is limited by the diffraction of light to about 200 nm laterally and 500 nm axially,[11] preventing diffraction-limited microscopy to resolve single molecules in cells and tissues with high target densities. Second, multiplexing of different molecular species is severely limited by the relatively broad emission spectrum of fluorophores, preventing the separation of more than about four dye-labeled species in the visible spectrum.[11] Third, there is a specific need to label molecules with binders, creating issues in terms of specificity, binder size, and labeling efficiency. In an ideal scenario, where fluorescence microscopy would become the prime tool for spatial omics, its resolution should be improved to the size of single proteins (e.g., 5 nm or better spatial resolution), multiplexing capabilities be enhanced to hundreds or even thousands of target species, and small efficient high-performance labeling reagents be developed.

To pave the route for spatial omics with fluorescence microscopy, researchers have started to make use of the sequence programmability of nucleic acids to develop DNA-barcoded imaging probes for improving the multiplexing aspect in fluorescence microscopy. We here focus on different strategies for DNA, RNA, and protein multiplexing using DNA-based labeling probes. These approaches can further be combined with state-of-the-art super-resolution modalities,[12–15] technically approaching spatial resolutions of better than 5 nm.[16–18]

4. Multiplexed Protein Detection Using Sequential Labeling and Fluorescence Imaging

Some of the earliest implementations of spectrally unlimited multiplexing use sequential antibody labeling, imaging, and removal of the antibody. Several studies have applied this approach for multiplexed imaging in formalin-fixed tissues and cultured cells.[19,20] In multiplexed cyclic immunofluorescence imaging, by repeated staining cycles of fluorophore-conjugated antibodies against two antigens, two-channel imaging, and extinguishing the fluorescence by chemical treatment, 61-plex imaging was achieved.[21] In an extension of this technique, called tissue-based cyclic immunofluorescence microscopy, four-channel imaging was implemented.[22] By iterative fluorophore-conjugated antibody labeling, four-channel fluorescence imaging, and extinguishing fluorescence, 60-plex images were obtained. Lately, there have been efforts to automate[23] sequential multiplexed super-resolution microscopy in order to routinely achieve >10 target multiplexing.

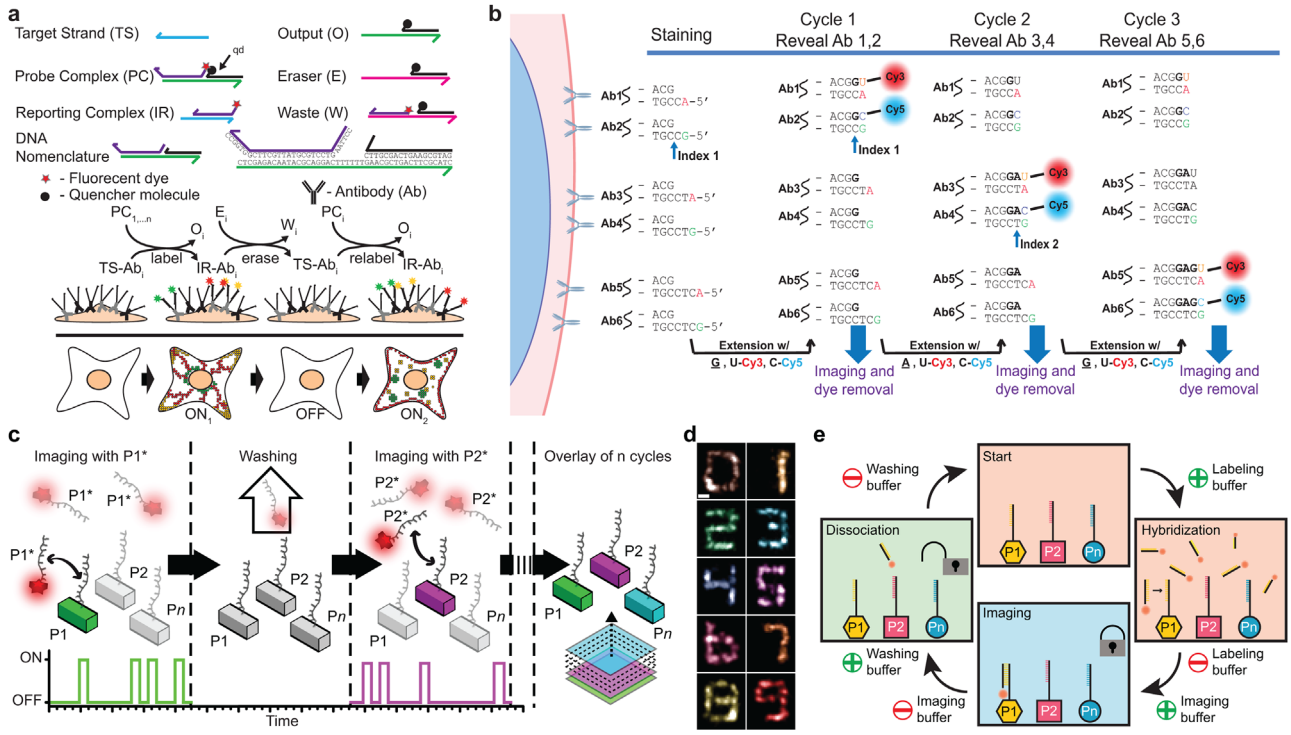

Figure 2. DNA-based multiplexing in fluorescence microscopy. a) Multiplexed in situ immunofluorescence labeling and sequential imaging of proteins using dynamic DNA complexes. The target strand (TS) is conjugated to an antibody against a protein of interest. Upon incubation of the sample with the probe complex (PC), the reporting complex (IR) is formed, unquenching the fluorescent dye, which is subsequently imaged. Post acquisition, an eraser strand (E) is incubated, which in turn removes the dye-labeled strand via toehold-mediated strand displacement from the target, concluding one imaging round. Next, another protein species can be labeled by introducing another set of probe complexes, repeating the imaging procedure. Adapted with permission.[25] Copyright 2012, Wiley. b) Co-detection by indexing (CODEX). Antibodies against targets of interest are labeled with a unique, rationally designed oligonucleotide duplex. In each cycle, they are extended by one out of two non-fluorescent indexing nucleotides (A or G), filling the index position across all antibodies. Exactly two DNA duplexes (and thus two target proteins) are furthermore fluorescently labeled by either Cy3 or Cy5 dyes based on their designed sequence, enabling their detection by fluorescence microscopy. Post-acquisition, the dyes are cleaved and washed away. The whole process is then repeated until all targets are visualized. Adapted with permission.[29] Copyright 2018, Elsevier. c) DNA-based multiplexing in super-resolution microscopy by Exchange-PAINT. Target species are simultaneously labeled with orthogonal, single-stranded DNA molecules (called "docking" strands). In the first round, a fluorescently labeled DNA oligo (termed "imager"), complimentary to the docking strand on the first target, is introduced and DNA-PAINT image acquisition is performed (see text for more details). Post acquisition, the transiently binding imager strands against the first target are washed out and imagers (carrying the same spectral dye) complementary to the second target strand are introduced. This process is then repeated iteratively until every target species is imaged. Adapted with permission.[17] Copyright 2017, Springer Nature. d) Exemplary ten-target in vitro Exchange-PAINT experiment on DNA origami structures, representing digits 0 to 9. Adapted with permission.[34] Copyright 2014, Springer Nature. e) Extension of the exchange concept to all fluorescence imaging modalities. Targets are labeled with orthogonal 12 nucleotide long DNA sequences, leading to quasi-stable imager-docking complexes. After hybridization, all probe strands remaining in solution are washed out and imaging is performed subsequently. Next, a washing buffer (containing formamide) is introduced to dissociate the probe strands from the target of interest. Finally, the washing buffer and the now diffusing probe strands are replaced by a labeling buffer, and the whole process is repeated until all target signals are acquired. Adapted with permission.[36] Copyright 2017, Wiley. Scale bar: 25 nm (d).

5. DNA-Barcoded Fluorescence Microscopy for Highly Multiplexed Protein Imaging

While cyclic immunofluorescence imaging—as described above—theoretically allows for unlimited multiplexing, there is a practical limit, as labeling, imaging, and dye inactivation is a time-consuming procedure, taking up to 24 h per imaging round.[21,22,24] DNA-based labeling and imaging approaches can be used to overcome this limitation. As a first example, we will discuss approaches from Michael Diehl's lab, who use dynamic DNA complexes to achieve multiplexed protein detection in cells, not limited by the use of spectrally distinct fluorophores or sequential staining procedures.[25–27] In their approach, multiple antibodies against different proteins of interest are conjugated with orthogonal single-stranded DNA molecules (called target strands), such that each target antibody carries a unique DNA barcode (**Figure 2**a). Post-fixation, cell samples are labeled with this antibody mix (simultaneously, rather than sequentially). Prior to image acquisition, a "probe complex" is flushed in, consisting of three DNA strands, where one carries a dye and another strand a quencher molecule, preventing fluorescence from the dye. By a toehold-mediated strand displacement reaction,[28] in which a single-stranded sequence extension is used as a nucleation motif for the target strand, the dye-labeled strand can be displaced from the probe complex (forming the "reporting complex"). This separates the dye from the quencher

strand, which (as an "output") can diffuse into the solution and eventually be washed away. In the next step, the reporting complex on the first species of interest can be visualized via classical fluorescence microscopy. Post-acquisition, an eraser stand is introduced, which displaces the fluorescently labeled strand from the target, forming a "waste complex". After washing out the waste complex, the system is in the initial state and the process can be repeated iteratively for all remaining targets. It is of importance to note that this sequential labeling and imaging approach also overcomes the limitation of spectral multiplexing, as in each round the same spectral dyes (e.g., three species per round) can be reused in subsequent rounds.

Another implementation that makes use of DNA-conjugated antibodies for multiplexed protein imaging with fluorescence microscopy is called co-detection by indexing (CODEX), developed by Garry Nolan's lab.[29] In CODEX (Figure 2b), the DNA barcode strands are hybridized with complementary "primer" strands. In the first round, the primer on the protein to be imaged is extended by a DNA polymerase with a single dye-labeled nucleotide. Simultaneously, the DNA barcode on the protein species to be imaged in the second round is extended by a nucleotide. Post-acquisition of round one, the fluorophore is extinguished. By repeating primer extension, imaging, and inactivation of the fluorophore, CODEX was thus far able to acquire as many as 22 different proteins of interest in mouse-isolated splenocyte cells.

6. DNA-Based Super-Resolution Microscopy

As discussed before, in the most ideal implementation of spatial omics by fluorescence microscopy, the resolution should approach the size of single proteins. To circumvent the classical diffraction limit in fluorescence microscopy, super-resolution techniques have been invented.[12–14] One prominent approach is called single molecule localization microscopy (SMLM),[30,31] where super-resolution is achieved by spatiotemporal separation of single-molecule emission and subsequent sub-diffraction localization. In DNA points accumulation in nanoscale topography (DNA-PAINT),[32] the necessary switching between ON- and OFF-states is achieved by diffusion and transient binding of short dye-labeled oligonucleotides (called "imager" strands) to their respective target-bound complementary strands (called "docking" strands). To implement DNA- or Exchange-PAINT for imaging cellular targets such as proteins, typically antibodies, nanobodies, or small molecules binders such as phalloidin for actin imaging are functionalized with DNA-PAINT docking sequences using standard biochemical conjugation assays.[33] As dye-labeled imager strands bind only transiently to their targets, spectrally unlimited multiplexing by sequential imaging of complementary target strands can be achieved by using the unique sequence specificity of DNA molecules. This concept is called Exchange-PAINT[34] (Figure 2c). Here, different target species are labeled with orthogonal, single-stranded DNA molecules. For imaging of the first target, the imager complementary to the docking strand bound to this first target is washed in. After image acquisition, the imager strands are washed out and a second imager species, complementary to docking strands bound to the second target are introduced. This process is then repeated until all target species are imaged. Figure 2d presents exemplary DNA origami in vitro data for ten-target Exchange-PAINT. Each digit represents one unique DNA origami species.

In DNA origami,[35] a long single-stranded DNA molecule (called "scaffold," usually derived from the genome of the bacteriophage M13mp18) is folded into a pre-designed shape by ≈200 short, complementary strands called "staples." Each staple specifically binds parts of the scaffold together in a thermal annealing process, folding the scaffold into the prescribed shape. These structures represent a unique class of self-assembled, fully addressable 12 × 18 pixel-sized "nano-breadboards," where "pixels" (i.e., single staple strands) are spaced 5 nm apart and can be designed to carry specific docking strands.[17] For applications where DNA origami structures are employed to label and detect nucleic acid sequences (such as, e.g., mRNA), origami can be equipped with unique single-stranded extensions, which can, for example, bind to specific RNA sequences. For protein detection, DNA- or RNA-based aptamers can be employed.

In Exchange-PAINT, similar to the DNA-barcoded imaging approaches discussed above, multiplexing capacity is only limited by the number of orthogonal DNA sequences (fulfilling certain criteria for binding kinetics compatible with DNA-PAINT). However, while approaches from Diehl and Nolan are relatively time consuming (i.e., involve several steps for target activation and inactivation), image acquisition in Exchange-PAINT is comparably fast, as dye-labeled strands only transiently bind their targets and are thus easily replaced by a simple buffer exchange reaction, which can be as fast as a few tens of seconds.

The concept of Exchange-PAINT was later generalized to other super-resolution and diffraction-limited techniques.[36] Here, the imager/docking strand duplex is designed to yield a stable, rather than transient interaction (Figure 2e). This virtually "labels" the target with a "fixed" dye strand. Post image acquisition, the dye-labeled strand is forced to dissociate from the target using a low salinity, formamide-containing washing buffer, which reduces the melting temperature of the duplex.[37,38] Finally, the washing buffer and the now unbound dye-labeled strands are replaced by the incubation buffer and the whole process is repeated until all targets are imaged. This concept, termed Universal Multiplexing by DNA Exchange, now brings DNA-barcoded and thus theoretically unlimited multiplexing to virtually any fluorescence imaging modality.

7. Spatiospectral Barcoding Using Designer DNA Probes

While the aforementioned DNA-barcoded multiplexing approaches enable spectrally unlimited imaging, acquisition time increases linearly with the number of target species. While this is of no concern for a few tens of targets, acquisition times become prohibitively long for hundreds or even more species. One way to improve the rather simple sequential imaging approach is the combination with prescribed spatial or spectral information (or both).

One exciting implementation of a geometrically encoded barcode is shown in **Figure 3**a. Here, mRNA species are hybridized with fluorophore-conjugated complementary single-stranded DNA molecules and imaged with fluorescence microscopy, a technique called single-molecule fluorescence in situ hybridization (smFISH). The length of the mRNA molecule allows for

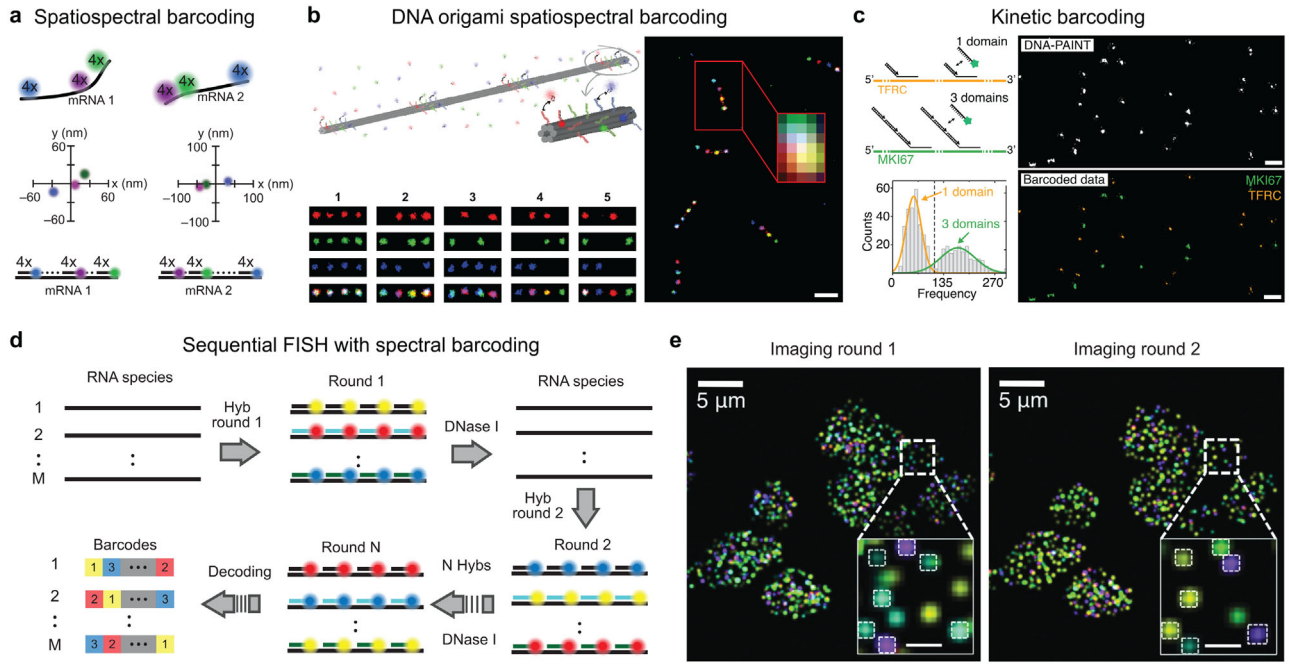

Figure 3. DNA-based combinatorial multiplexing. a) Spatiospectral barcoding for imaging a large number of nucleic acids. Schematics showing two RNA species labeled with three spectrally distinct fluorophores using a prescribed spatial arrangement. Based on the 2D-position of each of the fluorophores on a given RNA molecule, species can be identified. Adapted with permission.[39] Copyright 2012, Springer Nature. b) Self-assembled DNA origami-based spatiospectral barcodes (top left) visualized using Exchange-PAINT super-resolution microscopy (5 exemplary barcodes shown on the bottom left) enable sub-diffraction-sized barcoding for up to several thousand targets. Adapted with permission.[40] Copyright 2012, Springer Nature. c) Engineered binding kinetics for DNA-PAINT super-resolution imaging enables multiplexing of multiple RNA species. Two frequency barcodes are used in a proof-of-concept visualizing MKI67 and TFRC mRNA molecules. Based on the unique frequency of each RNA molecule obtained from a kinetic histogram analysis, a pseudo-color is assigned to each molecule. Adapted with permission.[41] Copyright 2019, American Chemical Society. d) Combinatorial multiplexing with sequential FISH (SeqFISH, exemplary codebook). The mRNA target is sequentially imaged by direct hybridization of a specific fluorophore conjugated to target-complementary DNA probes. By DNase I-catalyzed removal of the complements and subsequent hybridization of a new dye-labeled probe, a sequence-specific barcode can be assembled for each molecule of interest. e) Representative data showing two rounds of imaging in SeqFISH. Adapted with permission.[42] Copyright 2014, Springer Nature. Scale bars: 250 nm (b), 1 µm (c), 1 µm (e, inset).

the hybridization of several short DNA oligomers. This enables combinatorial labeling using spatially resolved barcodes. By implementing smFISH on mRNA species in *Saccharomyces cerevisiae*, Lubeck et al. performed multiplexed imaging by encoding the multi-target information in a spatial barcode.[39] In order to resolve sub-wavelength distances, these spatial barcodes were combined with orthogonal spectral information, enabling the identification of individual positions on sub-diffraction-sized RNA molecules. While spatial barcodes in principle represent a powerful and intuitive way to reach a high multiplexing capacity, the approach is hindered by relatively demanding requirements with regard to resolution in order to faithfully decode spatial information. More relaxed requirements are faced when implementing spectral barcodes. Using seven photoswitchable dyes and three dyes per barcode, Lubeck et al. were able to multiplex 32 mRNA species in a single round of imaging.

To overcome the possible ambiguity of spatial barcodes on flexible mRNA targets, recently developed self-assembled DNA origami structures can be employed as a solution to provide geometrically encoded labels (Figure 3b). Using 6-helix bundle structures, Lin et al. were able to use the unique spatial addressability and molecular stiffness of these structures to create sub-diffraction-sized spatiospectral barcodes consisting of, for example, five spatial positions, which can be "labeled" with either a blue, green, or red fluorophore, theoretically allowing for approx. 2400 barcode species (Figure 3b).[40] These nanobarcodes could, for example, be used for ex situ mRNA detection from cell lysates by modifying the DNA nanostructures with single-stranded capture sequences, complementary to an mRNA sequence of interest. Using seven spatial positions, the multiplexing capacity can be increased to theoretically over 800 000 possible targets, covering the transcriptome multiple times over. While this represents an exciting advance, the DNA origami-based spatial barcodes are only really applicable in ex situ imaging applications. The main reason for this is that—albeit nanoscale in size—the structures are still approximately 400 nm in length, preventing their applicability to target biomolecules in situ inside cells.

An entirely orthogonal approach for multiplexed, barcoded microscopy can be achieved by using the predictable, well-understood hybridization kinetics in DNA-PAINT microscopy to rationally design the blinking behavior (e.g., fluorescence ON- and OFF-times) of targets with engineered binding frequency and duration (Figure 3c).[41] This general concept uses the fact that a target exhibiting, for example, five DNA-PAINT binding sites compared to a target with one shows a five times higher blinking frequency. If these two frequency levels could be distinguished, they can then be used as a barcode. Figure 3c shows

a proof-of-concept implementation of such a frequency barcode using smFISH targeting two mRNA target species inside a cell. Here, the probe set against the MKI67 mRNA contains three concatenated binding sites per probe, while the set targeting TFRC contains only one binding site per probe. This can further be combined with a binding duration barcode (e.g., distinguishing the binding time and thus blink duration of a 9 versus 10 bp duplex) and spectral colors to considerably increase the amount of simultaneous detectable species (e.g., assuming four frequency levels and three spectral colors, one could acquire 124 target species simultaneously).

8. Genome-Scale Spatial Omics with Multiplexed Combinatorial Imaging

With the technical capability on the horizon to image hundreds or an even larger number of targets simultaneously in a single cell, target density becomes an increasingly severe problem, even for super-resolution implementations. When imaging a sparsely populated target, like in the case of the *S. cerevisiae* where all targeted mRNA species only occupied 2% of the cell volume, distinguishing signals from individual targets is relatively straightforward.[39] But for the case of a much more densely populated environment (or higher plex readout), individual species cannot be resolved. An elegant solution to this issue is to target only a subset of all targets in one imaging round. Instead of imaging all probes at once, the hybridized complements are displaced after a single imaging round by DNAse I treatment and the next subset of probes is hybridized. This introduces a sequential imaging pattern (SeqFISH),[42,43] in which the target is encoded by "positive" and "negative" readouts, a binary code (Figure 3d). These codes can then be visualized in a codebook, showing either all readout rounds ("positive" or "negative") or only the "positive," so called "barcoding" rounds. With this approach, it is possible to image F^N probes with F being the number of different fluorophores in a single round and N the total number of barcoding rounds (exemplary data, Figure 3e). By replacing the fixed dye on the FISH probes with a single-stranded overhang,[44] a secondary, dye-labeled complement can be hybridized, furthermore decoupling the "positive" readout signal from spectral colors as in Exchange-PAINT[34] and Universal Exchange.[36] When operating in densely populated environments, image correlation can be combined with the barcoding system to yield quantification even without single spot resolution.[45]

In a recent study, Eng et al. have shown that by using 60 such pseudocolors, they could image 10 000 mRNA species in mouse brain tissues (SeqFISH+).[46] In their barcoding approach, they separated the targets into three fluorescent channels and imaged 20 sequential rounds for each color channel, completing one superordinate barcoding round. Each target appears in exactly one of these 20 readout rounds. A total of four overarching barcoding rounds would theoretically allow for imaging 20^4 targets per fluorescent color, so in total an impressive number of 480 000 unique barcodes (**Figure 4**a).

With the complexity of barcodes rising, the inevitable question is: How error-prone is the coding strategy? In the case of SeqFISH, one additional round of imaging with specific targets was used to check for the most likely error, which is missing a hybridization event,[47] as a re-occurrence of misidentifications should be unlikely due to the use of DNAse I as "quencher." While this approach serves as an easy-to-implement and fast correction, another technique has set out to use "perfect codes" for the introduction of an error-robust encoding scheme to correct for a larger variety of possible error modes. In Multiplexed Error-Robust FISH (MERFISH),[48] Chen et al. have developed a codebook in which every target is encoded by a 16-bit binary barcode (Figure 4b). Using 16 rounds of imaging, the possible number of targets is $2^{16} - 1 = 65\,535$, yet misidentification and missing errors scale with the number of imaging rounds. This problem was solved by using a concept from information theory, called the Hamming distance (HD). Here, each barcode is separated from all others by at least four changes in binaries (HD4-code). This allows for the correction of one-bit errors and for the identification of two-bit errors. Furthermore, Chen et al. set the numbers of positive readouts per single barcode to four. With this decrease in positive readout bits, the signal per single round of imaging is kept low and it also accounts for the higher likelihood of missing a positive event ($1 \rightarrow 0$) than misidentification of background spots ($0 \rightarrow 1$). Nevertheless, with these boundaries, the number of targets drastically decreases from 65 535 to 140. By moving from an HD4- to an HD2-code, error-correction is lost (yet detection still possible), but in 14 rounds of imaging, Chen et al. were able to image 1001 mRNA targets. In a recent study, MERFISH was combined with expansion microscopy to image 10 000 mRNA targets using a 69-bit HD4 code with three colors and 23 rounds of hybridization and imaging.[49]

Apart from multiplexing different mRNA species, it is also possible to use the specificity of FISH to address multiplexed super-resolution imaging of chromosome conformation. Since the structural organization of chromatin is typically investigated by Hi-C approaches, providing ensemble average information without visualization, detailed high-resolution images from single-cell chromatin sub-structures are missing. Furthermore, chemical cross-linking is blind to physically separated fragments, thus preventing Hi-C to capture interactions if two fragments have just separated. These challenges were recently solved by implementing combinatorial 3D multiplexed super-resolution imaging of certain chromosome regions.[50] To image a 1.2 Mb chromosome region, Bintu et al. first divided it into consecutive segments of 30 kb. Each segment was then labeled with approximately 300 primary probes, to which secondary probes could be hybridized for sequential imaging.[44] After each imaging step, the probes were removed by either displacement or photobleaching. With this approach, the authors generated contact frequency maps for 250 chromosomes, which showed high agreement with previous Hi-C studies for the same region and additionally provided information about single-cell variability with high spatial resolution.

9. Outlook and Future Challenges

Zooming out, technology development on the side of spatial transcriptomics and genomics using fluorescence microscopy has yielded impressive advancements in the past years, now allowing to spatially visualize hundreds to thousands of nucleic acid species simultaneously in a single cell. Porting this unique capability to spatial proteomics would be an exciting next step, eventually closing the gap with MS-based proteomics techniques in

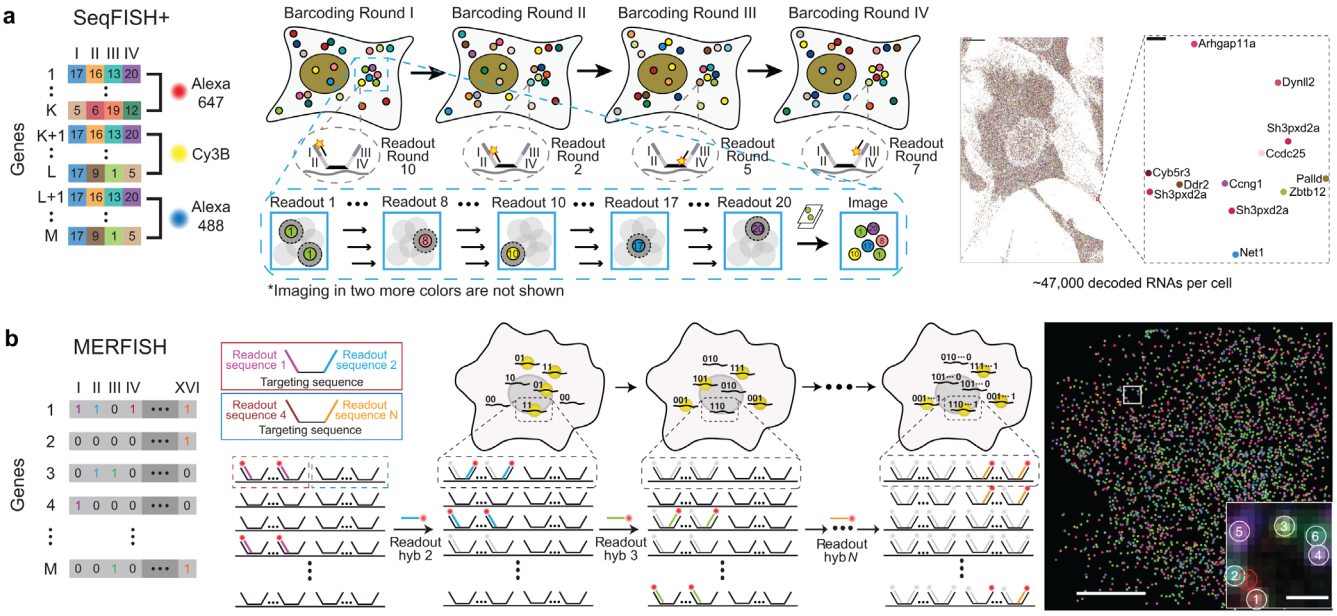

Figure 4. Error-robust spatial transcriptomics by SeqFISH+ and MERFISH. a) High-throughput combinatorial multiplexing with SeqFISH+. mRNA targets (1 to M) are assigned a unique code, consisting of four barcoding rounds (I to IV). The primary DNA probes consist of an RNA targeting sequence and single-stranded extensions for hybridization of four unique secondary probes (corresponding to the four barcoding rounds). In each barcoding round, 20 sequential labeling and readouts are performed (using three spectral colors, e.g., Alexa 488, Cy3B, Alexa 647). Each target is read out once per barcoding round. Data is shown for 47 000 decoded RNAs per cell. Adapted with permission.[46] Copyright 2019, Springer Nature. b) Multiplexed error robust FISH (MERFISH). Each mRNA target (1 to M) is assigned a binary barcode (16-bit in this example, using a modified Hamming distance codebook for error detection and correction), whose length corresponds to the number of sequential labeling and readout rounds. Each target is read out four times (corresponding to four 1 bits and twelve 0 bits). An exemplary imaging result coding for 140 RNA species in a cell is shown on the right. Adadpted with permission.[48] Copyright 2015, American Association for the Advancement of Science. Scale bars: 10 μm (a), 100 nm (a, inset), 10 μm (b), 1 μm (b, inset).

terms of content. MS-based techniques provide the unique advantage of de novo capturing whole protein contents as it is intrinsically a label-free method. However, recent developments on the side of fluorescence detection of RNA species without the use of FISH-based labels have opened exciting new routes, mainly fueled by the invention of the so-called fluorescence in situ sequencing approaches, or fluorescent in situ sequencing (FISSEQ).[51]

Translating spatiospectral combinatorial FISH-based barcoding approaches or FISSEQ to proteins, however, faces similar issues to the ones discussed in the imaging cytometry section of this review, which is the lack of small, efficient, and specific labeling probes for a large variety of protein species. Furthermore, while it is relatively economical and straightforward to synthesize and hybridize labeling probes for DNA and RNA targets,[52] a similar universal approach is missing for labeling proteins, which is traditionally achieved by antibodies. These can be up to two orders of magnitude more expensive than DNA probes in FISH experiments and especially for densely packed target proteins, the labeling efficiency can decrease due to sterical hindrance caused by the relatively large size of the antibody (usually approx. 150 kDa).[53,54] Furthermore, antibodies need to be screened for their suitability in immunofluorescence, which is a costly, tedious, and time-consuming effort. One of the reasons is that the fixation step (preserving the spatial state of the cell) is usually performed prior to immunolabeling. In order to address these difficulties and obtain improved labeling probes for proteins, especially for super-resolution microscopy techniques, multiple small high-affinity binders (e.g., aptamers, nanobodies, and affimers) have been developed.[33,53,55–57] Latest developments in this regard are slow off-rate modified aptamers (SOMAmer) for DNA-PAINT.[58] SOMAmers are small (7–30 kDa), quantitative, and versatile labeling probes and represent a unique class of DNA aptamers that contain modified bases with hydrophobic residues, similar to the amino acid residues abundant in antibody epitopes used for high-specificity and high-affinity binding of proteins. These base modifications increase the range of protein targets for which high-affinity ligands can be selected using traditional in vitro selection procedures. Since SOMAmers are synthetically produced, they are relatively cheap to fabricate once a suitable binder sequence is obtained. Lately, there have been multiple cellular applications of DNA-PAINT exploring protein pattern distributions of, for example, cell surface receptors such as members of the fibroblast growth factor receptor family,[59] spatial distributions of epidermal growth factor receptor (EGFR) and MET receptors[60] and relative spatial arrangements of EGFR, Her2, ErbB3, and c-Met receptors.[61] In order to further improve detection of low abundance targets in, for example, tissues with DNA-barcoded labeling reagents, recently developed signal amplification methods such as immuno-signal amplification by exchange reaction (SABER)[62] could be employed. In immuno-SABER, single-stranded DNA concatemers aggregate a multitude of short complementary fluorescently labeled strands per DNA-barcoded affinity reagent, thus

amplifying its signal. Furthermore, reducing the image voxel size by super-resolution microscopy is essential for the investigation of high-density targets in spatial omics. For imaging tens, potentially hundreds of rounds, a critical aspect in this regard is the amount of time spent for one round of imaging.[63–65] While super-resolution methods offer high spatial resolution, they are comparably slow. However, recently the imaging speed of DNA-PAINT was increased by one order of magnitude by rational DNA sequence design and optimized salinity of the imaging solution.[66] With further future advancements and possible combination with combinatorial barcoding schemes, spatial proteomics by super-resolution fluorescence microscopy might finally become a reality.

Acknowledgements

The authors thank Juanita Lara-Gutiérrez for helpful discussions. This work was supported in part by the DFG through an Emmy Noether Fellowship (DFG JU 2957/1-1) and the SFB 1032 (Nanoagents for the spatiotemporal control of molecular and cellular reactions, project A11), the ERC through an ERC Starting Grant (MolMap, Grant agreement number 680241), the Max Planck Society, the Max Planck Foundation, and the Center for Nanoscience (CeNS). F.S. acknowledges support from the SFB1032 graduate school. E.M.U. acknowledges support from the International Max Planck Research School for Molecular and Cellular Life Sciences (IMPRS-LS). M.G. acknowledges funding from the European Union's Horizon 2020 research and innovation programme under the Marie Skłodowska-Curie grant agreement no. 796606.

Open access funding enabled and organized by Projekt DEAL.

Conflict of Interest

The authors declare no conflict of interest.

Keywords

DNA nanotechnology, fluorescence microscopy, high-content imaging, multiplexing, super-resolution microscopy

Received: April 14, 2020
Revised: July 24, 2020
Published online: October 26, 2020

[1] N. G. Walter, C.-Y. Huang, A. J. Manzo, M. A. Sobhy, *Nat. Methods* **2008**, *5*, 475.
[2] T. T. Torres, M. Metta, B. Ottenwälder, C. Schlötterer, *Genome Res.* **2008**, *18*, 172.
[3] S. Brenner, M. Johnson, J. Bridgham, G. Golda, D. H. Lloyd, D. Johnson, S. Luo, S. McCurdy, M. Foy, M. Ewan, R. Roth, D. George, S. Eletr, G. Albrecht, E. Vermaas, S. R. Williams, K. Moon, T. Burcham, M. Pallas, R. B. DuBridge, J. Kirchner, K. Fearon, J. Mao, K. Corcoran, *Nat. Biotechnol.* **2000**, *18*, 630.
[4] R. Aebersold, M. Mann, *Nature* **2016**, *537*, 347.
[5] E. Lundberg, G. H. H. Borner, *Nat. Rev. Mol. Cell Biol.* **2019**, *20*, 285.
[6] C. Giesen, H. A. O. Wang, D. Schapiro, N. Zivanovic, A. Jacobs, B. Hattendorf, P. J. Schüffler, D. Grolimund, J. M. Buhmann, S. Brandt, Z. Varga, P. J. Wild, D. Günther, B. Bodenmiller, *Nat. Methods* **2014**, *11*, 417.
[7] M. Angelo, S. C. Bendall, R. Finck, M. B. Hale, C. Hitzman, A. D. Borowsky, R. M. Levenson, J. B. Lowe, S. D. Liu, S. Zhao, Y. Natkunam, G. P. Nolan, *Nat. Med.* **2014**, *20*, 436.
[8] B. Bodenmiller, *Cell Syst.* **2016**, *2*, 225.
[9] M. Uhlén, E. Björling, C. Agaton, C. A.-K. Szigyarto, B. Amini, E. Andersen, A.-C. Andersson, P. Angelidou, A. Asplund, C. Asplund, L. Berglund, K. Bergström, H. Brumer, D. Cerjan, M. Ekström, A. Elobeid, C. Eriksson, L. Fagerberg, R. Falk, J. Fall, M. Forsberg, M. G. Björklund, K. Gumbel, A. Halimi, I. Hallin, C. Hamsten, M. Hansson, M. Hedhammar, G. Hercules, C. Kampf, *Mol. Cell. Proteomics* **2005**, *4*, 1920.
[10] M. Uhlén, L. Fagerberg, B. M. Hallström, C. Lindskog, P. Oksvold, A. Mardinoglu, Å. Sivertsson, C. Kampf, E. Sjöstedt, A. Asplund, I. Olsson, K. Edlund, E. Lundberg, S. Navani, C. A.-K. Szigyarto, J. Odeberg, D. Djureinovic, J. O. Takanen, S. Hober, T. Alm, P.-H. Edqvist, H. Berling, H. Tegel, J. Mulder, J. Rockberg, P. Nilsson, J. M. Schwenk, M. Hamsten, K. Von Feilitzen, M. Forsberg, L. Persson, F. Johansson, M. Zwahlen, G. Von Heijne, J. Nielsen, F. Ponten, *Science* **2015**, *347*, 1260419.
[11] J. Pawley, *Handbook of Biological Confocal Microscopy*, 3rd ed., Springer Science & Business Media, Berlin **2013**.
[12] M. J. Rust, M. Bates, X. Zhuang, *Nat. Methods* **2006**, *3*, 793.
[13] E. Betzig, G. H. Patterson, R. Sougrat, O. W. Lindwasser, S. Olenych, J. S. Bonifacino, M. W. Davidson, J. Lippincott-Schwartz, H. F. Hess, *Science* **2006**, *313*, 1642.
[14] S. W. Hell, J. Wichmann, *Opt. Lett.* **1994**, *19*, 780.
[15] S. J. Sahl, S. W. Hell, S. Jakobs, *Nat. Rev. Mol. Cell Biol.* **2017**, *18*, 685.
[16] M. Dai, R. Jungmann, P. Yin, *Nat. Nanotechnol.* **2016**, *11*, 798.
[17] J. Schnitzbauer, M. T. Strauss, T. Schlichthaerle, F. Schueder, R. Jungmann, *Nat. Protoc.* **2017**, *12*, 1198.
[18] F. Balzarotti, Y. Eilers, K. C. Gwosch, A. H. Gynnå, V. Westphal, F. D. Stefani, J. Elf, S. W. Hell, *Science* **2017**, *355*, 606.
[19] C. Wählby, F. Erlandsson, E. Bengtsson, A. Zetterberg, *Cytometry* **2002**, *47*, 32.
[20] D. Pirici, L. Mogoanta, S. Kumar-Singh, I. Pirici, C. Margaritescu, C. Simionescu, R. Stanescu, *J. Histochem. Cytochem.* **2009**, *57*, 567.
[21] M. J. Gerdes, C. J. Sevinsky, A. Sood, S. Adak, M. O. Bello, A. Bordwell, A. Can, A. Corwin, S. Dinn, R. J. Filkins, D. Hollman, V. Kamath, S. Kaanumalle, K. Kenny, M. Larsen, M. Lazare, Q. Li, C. Lowes, C. C. Mcculloch, E. Mcdonough, M. C. Montalto, Z. Pang, J. Rittscher, A. Santamaria-Pang, B. D. Sarachan, M. L. Seel, A. Seppo, K. Shaikh, Y. Sui, J. Zhang, F. Ginty, *Proc. Natl. Acad. Sci. U. S. A.* **2013**, *110*, 11982.
[22] J.-R. Lin, B. Izar, S. Wang, C. Yapp, S. Mei, P. M. Shah, S. Santagata, P. K. Sorger, *eLife* **2018**, *7*, e31657.
[23] M. Klevanski, F. Herrmannsdoerfer, S. Sass, V. Venkataramani, M. Heilemann, T. Kuner, *Nat. Commun.* **2020**, *11*, 1552.
[24] J.-R. Lin, M. Fallahi-Sichani, P. K. Sorger, *Nat. Commun.* **2015**, *6*, 8390.
[25] R. M. Schweller, J. Zimak, D. Y. Duose, A. A. Qutub, W. N. Hittelman, M. R. Diehl, *Angew. Chem., Int. Ed. Engl.* **2012**, *51*, 9292.
[26] D. Y. Duose, R. M. Schweller, J. Zimak, A. R. Rogers, W. N. Hittelman, M. R. Diehl, *Nucleic Acids Res.* **2012**, *40*, 3289.
[27] J. Zimak, R. M. Schweller, D. Y. Duose, W. N. Hittelman, M. R. Diehl, *ChemBioChem* **2012**, *13*, 2722.
[28] B. Yurke, A. J. Turberfield, A. P. Mills Jr., F. C. Simmel, J. L. Neumann, *Nature* **2000**, *406*, 605.
[29] Y. Goltsev, N. Samusik, J. Kennedy-Darling, S. Bhate, M. Hale, G. Vazquez, S. Black, G. P. Nolan, *Cell* **2018**, *174*, 968.e15.
[30] B. Huang, M. Bates, X. Zhuang, *Annu. Rev. Biochem.* **2009**, *78*, 993.
[31] M. Sauer, M. Heilemann, *Chem. Rev.* **2017**, *117*, 7478.
[32] R. Jungmann, C. Steinhauer, M. Scheible, A. Kuzyk, P. Tinnefeld, F. C. Simmel, *Nano Lett.* **2010**, *10*, 4756.
[33] S. S. Agasti, Y. Wang, F. Schueder, A. Sukumar, R. Jungmann, P. Yin, *Chem. Sci.* **2017**, *8*, 3080.

[34] R. Jungmann, M. S. Avendaño, J. B. Woehrstein, M. Dai, W. M. Shih, P. Yin, *Nat. Methods* **2014**, *11*, 313.
[35] P. W. K. Rothemund, *Nature* **2006**, *440*, 297.
[36] F. Schueder, M. T. Strauss, D. Hoerl, J. Schnitzbauer, T. Schlichthaerle, S. Strauss, P. Yin, H. Harz, H. Leonhardt, R. Jungmann, *Angew. Chem., Int. Ed. Engl.* **2017**, *56*, 4052.
[37] T. Liedl, F. C. Simmel, *Anal. Chem.* **2007**, *79*, 5212.
[38] R. Jungmann, T. Liedl, T. L. Sobey, W. Shih, F. C. Simmel, *J. Am. Chem. Soc.* **2008**, *130*, 10062.
[39] E. Lubeck, L. Cai, *Nat. Methods* **2012**, *9*, 743.
[40] C. Lin, R. Jungmann, A. M. Leifer, C. Li, D. Levner, G. M. Church, W. M. Shih, P. Yin, *Nat. Chem.* **2012**, *4*, 832.
[41] O. K. Wade, J. B. Woehrstein, P. C. Nickels, S. Strauss, F. Stehr, J. Stein, F. Schueder, M. T. Strauss, M. Ganji, J. Schnitzbauer, H. Grabmayr, P. Yin, P. Schwille, R. Jungmann, *Nano Lett.* **2019**, *19*, 2641.
[42] E. Lubeck, A. F. Coskun, T. Zhiyentayev, M. Ahmad, L. Cai, *Nat. Methods* **2014**, *11*, 360.
[43] C.-H. L. Eng, S. Shah, J. Thomassie, L. Cai, *Nat. Methods* **2017**, *14*, 1153.
[44] B. J. Beliveau, A. N. Boettiger, M. S. Avendaño, R. Jungmann, R. B. McCole, E. F. Joyce, C. Kim-Kiselak, F. Bantignies, C. Y. Fonseka, J. Erceg, M. A. Hannan, H. G. Hoang, D. Colognori, J. T. Lee, W. M. Shih, P. Yin, X. Zhuang, C.-T. Wu, *Nat. Commun.* **2015**, *6*, 7147.
[45] A. F. Coskun, L. Cai, *Nat. Methods* **2016**, *13*, 657.
[46] C.-H. L. Eng, M. Lawson, Q. Zhu, R. Dries, N. Koulena, Y. Takei, J. Yun, C. Cronin, C. Karp, G.-C. Yuan, L. Cai, *Nature* **2019**, *568*, 235.
[47] S. Shah, E. Lubeck, W. Zhou, L. Cai, *Neuron* **2016**, *92*, 342.
[48] K. H. Chen, A. N. Boettiger, J. R. Moffitt, S. Wang, X. Zhuang, *Science* **2015**, *348*, aaa6090.
[49] C. Xia, J. Fan, G. Emanuel, J. Hao, X. Zhuang, *Proc. Natl. Acad. Sci. U. S. A.* **2019**, *116*, 19490.
[50] B. Bintu, L. J. Mateo, J.-H. Su, N. A. Sinnott-Armstrong, M. Parker, S. Kinrot, K. Yamaya, A. N. Boettiger, X. Zhuang, *Science* **2018**, *362*, eaau1783.
[51] J. H. Lee, E. R. Daugharthy, J. Scheiman, R. Kalhor, J. L. Yang, T. C. Ferrante, R. Terry, S. S. F. Jeanty, C. Li, R. Amamoto, D. T. Peters, B. M. Turczyk, A. H. Marblestone, S. A. Inverso, A. Bernard, P. Mali, X. Rios, J. Aach, G. M. Church, *Science* **2014**, *343*, 1360.
[52] B. J. Beliveau, E. F. Joyce, N. Apostolopoulos, F. Yilmaz, C. Y. Fonseka, R. B. McCole, Y. Chang, J. B. Li, T. N. Senaratne, B. R. Williams, J.-M. Rouillard, C.-T. Wu, *Proc. Natl. Acad. Sci. U. S. A.* **2012**, *109*, 21301.
[53] T. Schlichthaerle, A. S. Eklund, F. Schueder, M. T. Strauss, C. Tiede, A. Curd, J. Ries, M. Peckham, D. C. Tomlinson, R. Jungmann, *Angew. Chem., Int. Ed. Engl.* **2018**, *57*, 11060.
[54] D. Virant, B. Traenkle, J. Maier, P. D. Kaiser, M. Bodenhöfer, C. Schmees, I. Vojnovic, B. Pisak-Lukáts, U. Endesfelder, U. Rothbauer, *Nat. Commun.* **2018**, *9*, 930.
[55] F. Opazo, M. Levy, M. Byrom, C. Schäfer, C. Geisler, T. W. Groemer, A. D. Ellington, S. O. Rizzoli, *Nat. Methods* **2012**, *9*, 938.
[56] J. Ries, C. Kaplan, E. Platonova, H. Eghlidi, H. Ewers, *Nat. Methods* **2012**, *9*, 582.
[57] T. Schlichthaerle, M. T. Strauss, F. Schueder, A. Auer, B. Nijmeijer, M. Kueblbeck, V. J. Sabinina, J. V. Thevathasan, J. Ries, J. Ellenberg, J. D. Carter, S. Gupta, N. Janjic, R. Jungmann, *Angew. Chem.* **2019**, *131*, 13138.
[58] S. Strauss, P. C. Nickels, M. T. Strauss, V. J. Sabinina, J. Ellenberg, J. D. Carter, S. Gupta, N. Janjic, R. Jungmann, *Nat. Methods* **2018**, *15*, 685.
[59] M. S. Schröder, M.-L. I. E. Harwardt, J. V. Rahm, Y. Li, P. Freund, M. S. Dietz, M. Heilemann, *Methods* **2020**, https://doi.org/10.1016/j.ymeth.2020.05.004.
[60] M.-L. I. E. Harwardt, M. S. Schröder, Y. Li, S. Malkusch, P. Freund, S. Gupta, N. Janjic, S. Strauss, R. Jungmann, M. S. Dietz, M. Heilemann, *Int. J. Mol. Sci.* **2020**, *21*, 2803.
[61] S. Strauss, R. Jungmann, *Nat. Methods* **2020**, *17*, 789.
[62] S. K. Saka, Y. Wang, J. Y. Kishi, A. Zhu, Y. Zeng, W. Xie, K. Kirli, C. Yapp, M. Cicconet, B. J. Beliveau, S. W. Lapan, S. Yin, M. Lin, E. S. Boyden, P. S. Kaeser, G. Pihan, G. M. Church, P. Yin, *Nat. Biotechnol.* **2019**, *37*, 1080.
[63] P. Almada, P. M. Pereira, S. Culley, G. Caillol, F. Boroni-Rueda, C. L. Dix, G. Charras, B. Baum, R. F. Laine, C. Leterrier, R. Henriques, *Nat. Commun.* **2019**, *10*, 1223.
[64] A. Archetti, E. Glushkov, C. Sieben, A. Stroganov, A. Radenovic, S. Manley, *Nat. Commun.* **2019**, *10*, 1267.
[65] F. Stehr, J. Stein, F. Schueder, P. Schwille, R. Jungmann, *Nat. Commun.* **2019**, *10*, 1268.
[66] F. Schueder, J. Stein, F. Stehr, A. Auer, B. Sperl, M. T. Strauss, P. Schwille, R. Jungmann, *Nat. Methods* **2019**, *16*, 1101.

Ralf Jungmann received his Ph.D. in physics from the Technical University Munich in 2010 working with Prof. Dr. Friedrich C. Simmel on DNA origami. From 2011 to 2014, he was a postdoctoral fellow at the Wyss Institute at Harvard University with Prof. Dr. Peng Yin and Prof. Dr. William Shih. Since 2015, he has headed an independent research group at the Max Planck Institute of Biochemistry and the Ludwig Maximilian University Munich supported by the Emmy Noether Program of the DFG. In 2016, he was appointed as associate professor at the LMU. His research focuses on the development of DNA-based super-resolution techniques and their application in cell biology and biomedicine.